Determination of Defect Concentrations in ^{28}Si Crystals Using EPR for the Realization of the Kilogram

Shigeki Mizushima, Naoki Kuramoto, and Takahide Umeda

***Abstract*— To realize the kilogram using the X-ray crystal density method, ^{28}Si crystals grown by the floating zone method were employed. Samples cut from two ^{28}Si crystals, the AVO28 crystal (Si28-10Pr11 crystal) and the Si28-23Pr11 crystal, were analyzed by means of an electron paramagnetic resonance (EPR) spectroscopy. The samples were prepared by mirror polishing and subsequent etching using tetramethylammonium hydroxide (TMAH) solution. TMAH etching eliminates signals from the mechanically damaged surface layers of amorphous silicon and allows for the observation of small signals from vacancy defects in bulk crystals. In the study, the signal level of the vacancy defects was below the detection limit of 1×10^{12} cm^{-3}, and the amount of vacancy correction required to realize the kilogram was estimated to be 0.00(23) μg for both ^{28}Si crystals. Therefore, it was concluded that the 39(21) μg inconsistency between the kilogram realizations achieved using the two ^{28}Si crystals reported thus far cannot be explained by the existence of vacancy defects that are EPR active in the dark or under illumination.**

***Index Terms*— Electron paramagnetic resonance (EPR), kilogram, measurement uncertainty, metrology, silicon crystal, vacancy defects.**

I. Introduction

THE kilogram is the base unit of mass in the International System of Units, and it has been defined by fixing the value of the Planck constant h as 6.626 070 15 $\times$ 10^{-34} J s [1]. Currently, there are two methods to realize the kilogram with the highest accuracy, namely, the X-ray crystal density (XRCD) method and the method of comparing electrical and mechanical power by means of the Kibble balances [2].

The National Metrology Institute of Japan (NMIJ) adopts the XRCD method to realize the kilogram [3]. The XRCD method utilizes spheres with a diameter of approximately 93.7 mm, which are produced from ^{28}Si crystals grown by the floating zone method. The number of ^{28}Si atoms in the sphere is counted by measuring the volume of the sphere and the lattice constant of the crystal. However, the counting of the total number of ^{28}Si atoms in the sphere can be affected by the presence of defects in the crystal. Therefore, the evaluation of the amount of defects in ^{28}Si crystals is essential for the realization of the kilogram with the highest accuracy.

In this context, several studies have been conducted to date on defects in silicon crystals to realize the kilogram. Deslattes and Kessler [4] reported the qualitative difference between a natural isotope ratio silicon crystal used by NMIJ (formerly the National Research Laboratory of Metrology) and that used by Physikalisch-Technische Bundesanstalt per the electron paramagnetic resonance (EPR) spectroscopy. Gebauer *et al.* [5] applied positron annihilation lifetime spectroscopy (PALS) to a silicon crystal grown by the floating zone method and found that the vacancy concentration in the crystal was in the range from 1×10^{14} to 4×10^{14} cm^{-3} by measuring more than 5×10^6 counts at a temperature ranging from 20 to 300 K. D'Agostino *et al.* [6] developed a method to measure the 10^{14} cm^{-3} vacancy concentration in silicon crystals with a few percentage uncertainty using Cu decoration and neutron activation.

In recent years, it has been estimated that the Avogadro constant determined using the Si28-23Pr11 crystal (produced in 2015) is smaller than that determined with the AVO28 crystal (Si28-10Pr11 crystal, produced from 2004 to 2007) by 3.9 $(2.1) \times 10^{-8}$ in terms of relative value [7]. This corresponds to a discrepancy of 39(21) μg for the realization of the kilogram. In this regard, it has been pointed out that the presence of undetected vacancies or self-interstitials could be a cause of the discrepancy. Another possible cause is that the mass of the oxide film and hydrocarbon contamination layer on the surface of silicon spheres may have been determined imperfectly by means of the surface analysis method [7]. If it is assumed that vacancies are responsible for the discrepancy, it must be noted that the AVO28 crystal contains more vacancies than the Si28-23Pr11 crystal by a concentration of 2×10^{15} cm^{-3}.

Against this backdrop, in this study, we used EPR spectroscopy to measure the concentration of vacancy defects in both crystals and investigated whether the vacancies in the crystals can explain this discrepancy. This article is an extension of the proceedings paper presented at the 2020 Conference on Precision Electromagnetic Measurements (CPEM) [8].

II. Measurement Method

As the details of the measurement method have already been reported [9], only a brief description is provided here.

Manuscript received August 27, 2020; revised January 31, 2021; accepted February 11, 2021. Date of publication February 24, 2021; date of current version March 15, 2021. This work was supported by the Japan Society for the Promotion of Science through a Grant-in-Aid for Scientific Research (C) under Grant 17K05112. The Associate Editor coordinating the review process was Richard L. Steiner. *(Corresponding author: Shigeki Mizushima.)*

Shigeki Mizushima and Naoki Kuramoto are with the National Metrology Institute of Japan (NMIJ), AIST, Tsukuba 305-8563, Japan (e-mail: s.mizushima@aist.go.jp).

Takahide Umeda is with the Institute of Applied Physics, University of Tsukuba, Tsukuba 305-8573, Japan.

Digital Object Identifier 10.1109/TIM.2021.3062186

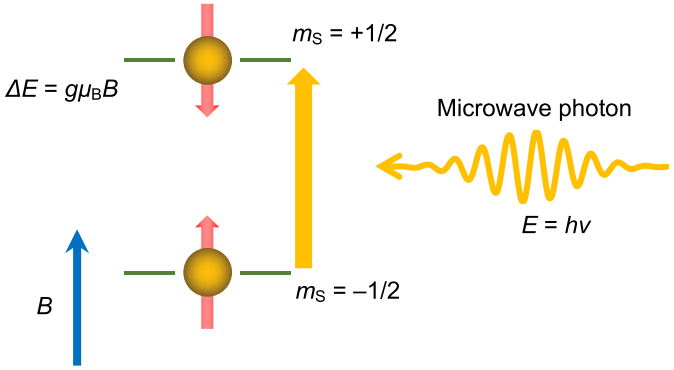

Fig. 1. Splitting of energy levels of an unpaired electron placed in magnetic field B and resonant absorption of microwave energy. Here, m_S represents the spin quantum number.

EPR detects unpaired electrons localized at the defects in a sample. The spectrum is recorded by sweeping an external magnetic field B under microwave irradiation with frequency ν. As shown in Fig. 1, the energy level of an unpaired electron placed in the magnetic field undergoes splitting; and resonance absorption occurs when $h\nu = g\mu_B B$, where h denotes the Planck constant, g the gyromagnetic factor (g factor), and μ_B the Bohr magneton.

Because the g factor of an unpaired electron localized at a defect deviates from that of a free electron due to spin-orbit coupling, it can be used to classify the defect. The effective g factor g_{eff} along a certain direction of the crystal can be described by the following equation upon selecting a certain Cartesian coordinate system:

$$g_{\text{eff}} = \left(g_x^2 \cos^2\theta_x + g_y^2 \cos^2\theta_y + g_z^2 \cos^2\theta_z\right)^{1/2}. \tag{1}$$

Here g_x, g_y, and g_z denote the principal values of the g factor, and $\cos\theta_x$, $\cos\theta_y$, and $\cos\theta_z$ the direction cosines of the magnetic field. When all three principal values are identical, the EPR center affords an "isotropic" signal independent of the magnetic field direction. Otherwise, the resulting EPR signal is "anisotropic."

In this regard, previous studies have identified the anisotropic EPR signals of vacancy defects in silicon crystals [10], [11]. For example, the g factor of positively charged single-vacancy defect V^+ in a silicon crystal is in the range of 1.9989–2.0087, and its EPR signal appears at a magnetic field given by the resonance condition depending on the microwave frequency. The simulation results of the EPR signals are available on the web-based database [12]. In this study, we focus on nine types of silicon crystal vacancy defects that have been identified by means of EPR, that is, charged vacancy defects ranging in size from a monovacancy defect to a pentavacancy defect, V^+, V^-, V_2^+, V_2^-, V_3^-, V_4^-, V_5^-, and monovacancy defects trapped by impurities, $(VO)^-$ and $(VP)^0$ [13].

The number of unpaired electrons localized at the defects was determined by comparing with a reference sample with a known number of unpaired electrons. We used a $CuSO_4 \cdot 5H_2O$ crystal that retains one unpaired electron per molecule as the reference sample. The number of unpaired electrons localized at the defects in a test sample, n_X, is given by the following equation:

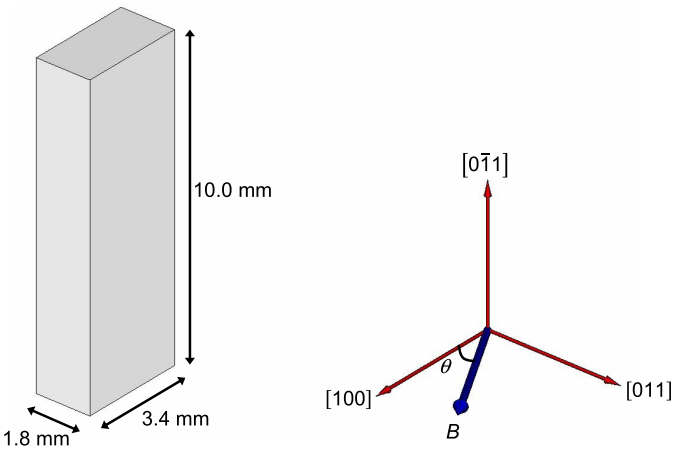

Fig. 2. Dimensions and orientation of a sample for EPR spectroscopy. Magnetic field B rotates in the plane perpendicular to the [0$\bar{1}$1] direction. Symbol θ denotes the angle between magnetic field B and the [100] direction.

$$n_X = f(A_X/A_R)(T_X/T_R)n_R \tag{2}$$

where f denotes the coefficient compensating for the decrease in sensitivity as a sample shifts from the center of a cavity resonator, (A_X/A_R) is the signal intensity ratio between the test and reference samples, (T_X/T_R) is the absolute temperature ratio between the test and reference samples, and n_R is the number of unpaired electrons in the reference sample.

All EPR measurements were performed using a Bruker E500 X-band spectrometer equipped with a Bruker ER4122SHQ cavity resonator (loaded Q-factor $Q_L \sim 10^5$). The sample temperature was stabilized using an Oxford ESR900 He-flow cryostat. The standard magnetic field modulation technique was used at a frequency of 100 kHz with a modulation width of 0.1 mT.

In the setup, a sample can be illuminated by a 100-W halogen lamp through a quartz glass rod, on which the sample is mounted. The illumination produces electron-hole pairs in the silicon crystal, providing additional unpaired electrons, and reveals defects that cannot be detected by EPR spectroscopy in the dark.

III. Sample Preparation

The samples used for EPR spectroscopy in this study were cut from the AVO28 crystal and the Si28-23Pr11 crystal grown by the floating zone method [7]. Table I lists the positions of the samples in the crystal boules. As shown in Fig. 2, the samples have a solid rectangular shape with dimensions of approximately 1.8 mm × 3.4 mm × 10.0 mm. Each edge of the samples was aligned parallel to the [100], [011], or [0$\bar{1}$1] crystal orientations. To reduce the EPR signal from the defectson the sample surfaces after cutting, the surfaces were mirror polished. In addition, the mechanically damaged layers were removed by means of a chemical method. First, the native oxide layer on the sample surfaces was removed using buffered hydrofluoric acid, and, subsequently, the silicon sample surfaces were etched by means of tetramethylammonium hydroxide (TMAH) solution. The etching condition was

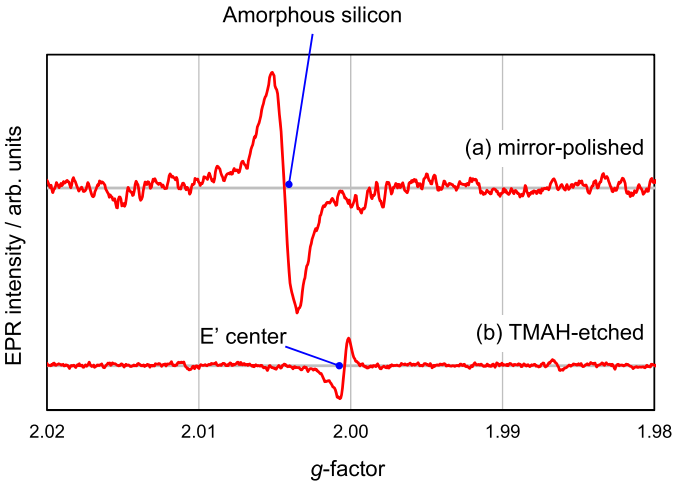

Fig. 3. First derivative EPR spectra measured at a microwave power $p = 2$ mW for the AVO28 crystal in the dark. (a) Sample with mirror-polished surfaces measured at a temperature of 25 K. (b) Sample with TMAH-etched surfaces measured at a temperature of 20 K. The angle θ between the magnetic field B and the [100] direction was set to 0°.

adjusted such that the thickness of the removed layer was approximately 2 μm.

IV. Measurement Results and Discussion

Fig. 3 compares the EPR spectrum for a sample with mirror-polished surfaces and that for a sample with TMAH-etched surfaces. Here we note that TMAH etching eliminates the previously reported broad isotropic signal ($g = 2.0055$) from defects in amorphous silicon ($Si_3 \equiv Si\bullet$, where the triple lines symbolize chemical bonds between atoms and the dot an unpaired electron) due to the mechanical damage of the mirror-polished surfaces [9]. This has made it possible to detect small anisotropic signals from various vacancy defects in silicon crystals, which is the main purpose of this research.

Fig. 4(a) and (b) shows the results of observing the AVO28 crystal at a temperature of 20 K with a microwave power of 2 mW in the dark and under illumination, respectively. First, the signals from the phosphorus impurity defects are noticeable, which has been well established by EPR measurements. This signal is characterized by a doublet hyperfine splitting due to the interaction between an electron and a phosphorus nuclear spin ($I = 1/2$). The concentration of the phosphorus impurity defects with unpaired electrons ($Si_4 = P\bullet$) is determined to be $0.14(2) \times 10^{12}$ cm^{-3} in the dark and $4.4(6) \times 10^{12}$ cm^{-3} under illumination. The observed signal is stronger under illumination than in the dark, thereby suggesting a relatively high concentration of compensation defects on the tail side of the AVO28 crystal. This finding is consistent with the relatively high boron impurity concentration of $344(28) \times 10^{12}$ cm^{-3} observed by infrared spectroscopy for a region near this sample [14].

Table II lists the measurement uncertainty evaluation for the concentration of phosphorus impurity defects with unpaired electrons under illumination for the AVO28 crystal. The main uncertainty sources were the uncertainty of EPR absorption intensity, nonuniform microwave magnetic field intensity, and difference in temperature between the reference and test

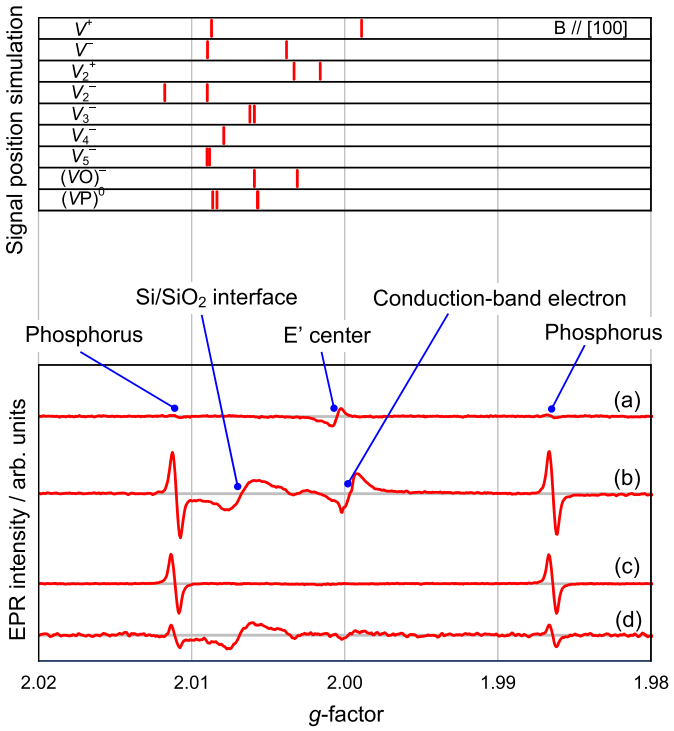

Fig. 4. First-derivative EPR spectra measured at a temperature of 20 K and microwave power $p = 2$ mW for the AVO28 crystal and the Si28-23Pr11 crystal. (a) AVO28 crystal in the dark. (b) AVO28 crystal under illumination. (c) Si28-23Pr11 crystal in the dark. (d) Si28-23Pr11 crystal under illumination. Angle θ between magnetic field B and the [100] direction was set to 0°. The simulation results of the signal positions for the nine different vacancy defects, which are based on g factors established by EPR measurements carried out by others during the period from 1955 to 2000 [13], are shown above.

samples. The concentration of phosphorus impurity defects with unpaired electrons under illumination was estimated to be 4.4×10^{12} cm^{-3}, and its relative standard uncertainty was estimated to be 0.15.

In addition, an isotropic signal from conduction band electrons, which were generated by illumination, was observed from the AVO28 crystal. We also observed an isotropic signal from the E' center ($O_3 \equiv Si\bullet$) in the dark. This signal may arise from the quartz glass parts, which were used for the sample rod and the liquid helium cryostat. Furthermore, anisotropic signals ($g = 2.0018$–2.0093) were observed under illumination. These signals were identified to originate from the P_b centers ($Si_3 \equiv Si\bullet$), which correspond to dangling bonds at the Si–SiO_2 interface, based on the g factor and angular dependence.

Fig. 4(c) and (d) shows the observation results of the Si28-23Pr11 crystal at a temperature of 20 K with a microwave power of 2 mW in the dark and under illumination, respectively. The concentration of phosphorus impurity defects with unpaired electrons is determined to be $2.6(4) \times 10^{12}$ cm^{-3} in the dark and $1.0(1) \times 10^{12}$ cm^{-3} under illumination. The observed signal is stronger in the dark than under illumination, which suggests that the Si28-23Pr11 crystal has a relatively low concentration of compensation defects. This result is consistent with the boron impurity concentration of $4.4(1.7) \times 10^{12}$ cm^{-3} as determined by infrared spectroscopy for a part of this sample [7].

TABLE I

POSITION OF SAMPLES IN CRYSTAL BOULES FOR EPR SPECTROSCOPY. THE SURFACES WERE ETCHED IN TMAH SOLUTION AFTER MIRROR POLISHING

Crystal name	Sample region	Axial distance from seed/mm	Radial distance from the center/mm
AVO28 crystal (Si28-10Pr11 crystal)	9.R1	~ 420	15.3
Si28-23Pr11 crystal	M.R2	~ 115	18.8

TABLE II

MEASUREMENT UNCERTAINTY EVALUATION FOR THE CONCENTRATION OF PHOSPHORUS IMPURITY DEFECTS WITH UNPAIRED ELECTRONS IN THE AVO28 CRYSTAL UNDER ILLUMINATION

Uncertainty component	Value	Relative standard uncertainty
Correction coefficient for the decrease in sensitivity, f	1.11	0.03
EPR absorption intensity from the test sample, A_X	1.06 arb. units	0.06
EPR absorption intensity from the reference sample, A_R	8.8919×10^6 arb. units	0.06
Absolute temperature of the test sample, T_X	20 K	0.02
Absolute temperature of the reference sample, T_R	298 K	0.004
Number of unpaired electrons in the reference sample, n_R	3.022×10^{19}	0.01
Difference in shape between reference and test samples in nonuniform microwave magnetic field B_1		0.06
Difference in position between reference and test samples in nonuniform microwave magnetic field B_1		0.06
Difference in transmission medium between reference and test samples for microwave magnetic field B_1		0.06
Significant difference in temperature between reference and test samples		0.06
Number of phosphorus atoms with unpaired electrons in the test sample, n_X	0.27×10^{12}	0.15
Volume of the test sample at 20 °C, V_S	0.0614 cm^3	7×10^{-5}
Concentration of phosphorus atoms with unpaired electrons in the test sample, c_X	4.4×10^{12} cm^{-3}	0.15

In addition, an isotropic signal from the conduction band electrons and anisotropic signals from P_b centers were observed as with the AVO28 crystal. The absence of the E' center signal in the spectrum observed for the Si28-23Pr11 crystal may be explained by the fact that the quartz glass parts of the liquid helium cryostat was replaced with a new one before measuring the Si28-23Pr11 crystal.

However, anisotropic signals from vacancy defects in the bulk crystal were not observed in the AVO28 crystal or the Si28-23Pr11 crystal in the expected range of the g factor. Therefore, we conclude that the concentrations of the nine types of vacancy defects in both crystals were below the detection limit of this measurement, 1×10^{12} cm^{-3}.

The estimations of the mass deficit of a 1-kg silicon sphere for the nine types of vacancy defects, V^+, V^-, V_2^+, V_2^-, V_3^-, V_4^-, V_5^-, $(VO)^-$, and $(VP)^0$ are listed in Table III. As the concentrations of the nine types of vacancy defects were below the detection limit of 1×10^{12} cm^{-3} in this measurement, the concentration of each defect was estimated to be 0.0×10^{12} cm^{-3}, and its corresponding standard uncertainty was estimated to be 0.6×10^{12} cm^{-3} upon assuming a uniform distribution of possible values of the concentration with a half-width of 1×10^{12} cm^{-3}, which is the value of the detection limit. The mass deficit of a 1-kg silicon sphere was subsequently derived using the fact that the density of ^{28}Si atoms in a crystal at a temperature of 20 °C is 4.99×10^{22} cm^{-3}. As a result, the total concentration of the nine types of vacancy defects was estimated to be $0.0(5.2) \times 10^{12}$ cm^{-3}, and the mass deficit of a 1-kg silicon sphere was estimated to be 0.00(23) μg.

To calculate the total concentration of the nine types of vacancy defects, the correlation coefficient between the measured concentrations of the nine types of vacancy defects was assumed to be +1. This is because the concentrations of the nine types of vacancy defects were below the detection limit as described above, and each corresponding uncertainty was assumed to be the uncertainty derived from the common quantity, i.e., the detection limit of the same measuring instrument.

Table IV summarizes the concentrations of the phosphorus impurity defects and vacancy defects obtained using EPR spectroscopy for the AVO28 crystal and the Si28-23Pr11 crystal. For the AVO28 crystal, the concentration of phosphorus defects with unpaired electrons was higher under

TABLE III

CONCENTRATIONS OF THE NINE TYPES OF VACANCY DEFECTS WITH UNPAIRED ELECTRONS AND THE CORRESPONDING MASS DEFICITS FOR A 1-kg ^{28}Si SINGLE CRYSTAL PRODUCED FROM THE AVO28 CRYSTAL AND THE Si28-23Pr11 CRYSTAL

Types of vacancy defect	g-factor when $\theta = 0°$	Concentration /(10^{12} cm^{-3})	Mass deficit for a 1-kg ^{28}Si single crystal/μg
V^+	1.9989, 2.0087	0.0(6)	0.00(1)
V^-	2.0038, 2.0090	0.0(6)	0.00(1)
V_2^+	2.0016, 2.0033	0.0(6)	0.00(2)
V_2^-	2.0090, 2.0118	0.0(6)	0.00(2)
V_3^-	2.0059, 2.0062	0.0(6)	0.00(3)
V_4^-	2.0079	0.0(6)	0.00(5)
V_5^-	2.0088, 2.0090	0.0(6)	0.00(6)
$(VO)^-$	2.0031, 2.0059	0.0(6)	0.00(1)
$(VP)^0$	2.0057, 2.0084, 2.0086	0.0(6)	0.00(1)
Total	---	0.0(5.2)	0.00(23)

To convert the concentration of vacancy defects to the mass deficit, we assumed that the number density of ^{28}Si atoms in a single crystal at 20 °C to be approximately 4.99×10^{22} cm^{-3}.

TABLE IV

CONCENTRATIONS OF DEFECTS WITH UNPAIRED ELECTRONS OBSERVED BY MEANS OF EPR SPECTROSCOPY. (a) CONCENTRATION OF PHOSPHORUS IMPURITY DEFECTS/10^{12} cm^{-3}. (b) TOTAL CONCENTRATION OF THE NINE TYPE VACANCY DEFECTS/10^{12} cm^{-3}

(a)

Measurement condition	AVO28 crystal	Si28-23Pr11 crystal
In the dark	0.14(2)	2.6(4)
Under illumination	4.4(6)	1.0(1)

(b)

Measurement condition	AVO28 crystal	Si28-23Pr11 crystal
In the dark	0.0(5.2)	0.0(5.2)
Under illumination	0.0(5.2)	0.0(5.2)

illumination than in the dark. On the other hand, for the Si28-23Pr11 crystal, the concentration of phosphorus defects with unpaired electrons was higher in the dark than under illumination. As described above, this disparity is explained by the difference in the concentration of boron impurities, which is a compensation defect in the crystals. Concerning the vacancy defects, EPR signals exceeding the detection limit of 1×10^{12} cm^{-3} were not observed for the AVO28 crystal and the Si28-23Pr11 crystal, resulting in the estimation of the concentration of vacancy defects of $0.0(5.2) \times 10^{12}$ cm^{-3} for both crystals, as mentioned above.

The cause of the difference in the measured vacancy defect concentration between the result obtained using EPR in this study and that of PALS for a silicon crystal grown by the floating zone method [5] is not clear. However, it is important to note that the lower detection limit of vacancy defect concentration using PALS under normal conditions is 1.5×10^{15} cm^{-3} [15]. On the other hand, as shown in this article, the lower detection limit of vacancy defect concentration by our EPR measurement is considered to be 1×10^{12} cm^{-3}, being around 1.5×10^3 times more sensitive than PALS under normal conditions.

V. CONCLUSION

The ^{28}Si crystals grown by the floating zone method are used to realize the kilogram by means of the XRCD method. The EPR measurements were performed on the AVO28 crystal and the Si28-23Pr11 crystal to determine the corrections for vacancy defects in crystals, which is necessary for the accurate realization of the kilogram. We drew the following conclusions.

1) Owing to TMAH etching, the broad EPR signal from the mechanically damaged surface layers of amorphous

silicon, which covers small signals from vacancy defects, was no longer observed.

2) Anisotropic signals were observed for the g factor range from 2.0018 to 2.0093 under illumination. These were identified as signals from the P_b centers, corresponding to dangling bonds existing at the Si–SiO_2 interface.
3) Signals from vacancy defects with concentrations exceeding 1×10^{12} cm^{-3} were not observed for both crystals. As a result, the corrections for vacancy defects necessary to realize the kilogram for both the AVO28 crystal and the Si28-23Pr11 crystal were evaluated to be 0.00(23) μg. Therefore, it is concluded that the discrepancy of 39(21) μg between the kilograms realized using the two crystals reported to date is not attributable to the presence of vacancy defects that are EPR active in the dark or under illumination.

ACKNOWLEDGMENT

Several subprocesses of the sample preparation process were performed in the clean room for analog–digital superconductivity (CRAVITY) of the National Institute of Advanced Industrial Science and Technology (AIST) and MicroNano Open Innovation Center (MNOIC). The sample cut from the AVO28 crystal was used as per the international agreement on the AVO28 crystal produced by the International Avogadro Coordination project. The sample cut from the Si28-23Pr11 crystal was used per an international cooperation initiative between Physikalisch-Technische Bundesanstalt (PTB, Germany) and National Metrology Institute of Japan (NMIJ) in the field of the kilogram realization.

REFERENCES

[1] *Bureau International des Poids et Mesures*, The International System of Units (SI), 2019, p. 131.
[2] C. C. F. Mass and R. Quantities, "Mise en pratique for the definition of the kilogram in the SI," in *Proc. Int. Syst. Units (SI)*, 2019.
[3] N. Kuramoto *et al.*, "Realization of the kilogram based on the Planck constant at NMIJ," *IEEE Trans. Instrum. Meas.*, vol. 66, no. 6, pp. 1267–1274, Jun. 2017.
[4] R. D. Deslattes and E. G. Kessler, "The molar volume of silicon: Discrepancies and limitations," *IEEE Trans. Instrum. Meas.*, vol. 48, no. 2, pp. 238–241, Apr. 1999.
[5] J. Gebauer, F. Rudolf, A. Polity, R. Krause-Rehberg, J. Martin, and P. Becker, "On the sensitivity limit of positron annihilation: Detection of vacancies in as-grown silicon," *Appl. Phys. A, Mater. Sci. Process.*, vol. 68, no. 4, pp. 411–416, Apr. 1999.
[6] G. D'Agostino, M. Di Luzio, G. Mana, L. Martino, M. Oddone, and C. P. Sasso, "Quantification of the void volume in single-crystal silicon," *Anal. Chem.*, vol. 88, no. 23, pp. 11678–11683, Dec. 2016.
[7] G. Bartl *et al.*, "A new ^{28}Si single crystal: Counting the atoms for the new kilogram definition," *Metrologia*, vol. 54, no. 5, pp. 693–715, Oct. 2017.
[8] S. Mizushima, N. Kuramoto, and T. Umeda, "Determination of defect concentrations in ^{28}Si crystals using EPR for the realization of the kilogram," in *Proc. Conf. Precis. Electromagn. Meas. (CPEM)*, Aug. 2020, pp. 1–2.
[9] S. Mizushima, N. Kuramoto, K. Fujii, and T. Umeda, "Electron paramagnetic resonance study on ^{28}Si single crystal for the future realization of the kilogram," *IEEE Trans. Instrum. Meas.*, vol. 68, no. 6, pp. 1879–1886, Jun. 2019.
[10] G. D. Watkins, "A review of EPR studies in irradiated silicon," in *Proc. 7th Int. Conf. Phys. Semiconductors*, Paris, France, 1964, pp. 97–113.
[11] Y.-H. Lee and J. W. Corbett, "EPR study of defects in neutron-irradiated silicon: Quenched-in alignment under ⟨110⟩-uniaxial stress," *Phys. Rev. B, Condens. Matter*, vol. 9, no. 10, pp. 4351–4361, May 1974.
[12] T. Umeda, S. Hagiwara, M. Katagiri, N. Mizuochi, and J. Isoya, "A Web-based database for EPR centers in semiconductors," *Phys. B, Condens. Matter*, vols. 376–377, pp. 249–252, Apr. 2006.
[13] C. A. J. Ammerlaan *et al.*, "Paramagnetic centers in silicon," in *Landolt-Börnstein Group III Condens. Matter*, vol. 41A2. Berlin, Germany: Springer-Verlag, 2002, pp. 244–308.
[14] B. Andreas *et al.*, "Counting the atoms in a ^{28}Si crystal for a new kilogram definition," *Metrologia*, vol. 48, no. 2, pp. S1–S13, Mar. 2011.
[15] R. Krause-Rehberg and H. S. Leipner, "Determination of absolute vacancy concentrations in semiconductors by means of positron annihilation," *Appl. Phys. A, Solids Surf.*, vol. 64, no. 5, pp. 457–466, May 1997.

Shigeki Mizushima was born in Toyama, Japan, in 1972. He received the B.S. and M.S. degrees in physics from The University of Tokyo, Tokyo, Japan, in 1995 and 1997, respectively.

He is currently with the National Metrology Institute of Japan, National Institute of Advanced Industrial Science and Technology, Tsukuba, Japan. His current research interests include electron paramagnetic resonance study on silicon crystals, mass measurement using a mass comparator, and gravity measurement using an absolute gravimeter.

Naoki Kuramoto was born in Kanagawa, Japan, in 1971. He received the B.S., M.S., and Ph.D. degrees in chemistry from Saga University, Saga, Japan, in 1993, 1995, and 1998, respectively.

From 1995 to 1998, he was a Research Fellow with the Japan Society for the Promotion of Science. From 1998 to 1999, he was with the Tokyo University of Agriculture and Technology, Tokyo, Japan. In 1999, he joined the National Metrology Institute of Japan/the National Institute of Advanced Industrial Science and Technology (NMIJ/AIST), Tsukuba, Japan. He developed an optical frequency-scanning-type laser interferometer for measuring the diameter of Si spheres. The Planck constant determined by Kuramoto *et al.* in 2017 was used as an input datum for the determination of the Planck constant in the present definition of the kilogram. He is currently the Leader of the Mass Standards Group. He also serves as the Coordinator of the International Avogadro Coordination (IAC) Project. His research interests include the development of new mass measurement principles based on the new definition of the kilogram.

Takahide Umeda received the B.E., M.E., and Ph.D. degrees from the University of Tsukuba, Tsukuba, Japan, in 1994, 1996, and 1999, respectively. His Ph.D. thesis focused on localized electronic states in solar-cell materials studied by electron spin resonance (ESR) spectroscopy.

From 1998 to 1999, he was a Doctoral and a Post-Doctoral Fellow with the Japan Society of Promotion of Science and investigated ESR spectroscopy on crystalline-silicon surfaces. From 1999 to 2003, he was a Researcher with Fundamental Research Laboratory and Silicon Systems Research Laboratory, NEC Corporation, Tokyo, Japan. Since 2003, he was an Associate Professor with the University of Tsukuba. Since 2010, he has been with the Faculty of Pure and Applied Sciences, University of Tsukuba. His current specialty is magnetic resonance spectroscopy on defects and impurities in semiconductors and semiconductor devices, e.g., silicon and its large-scaled integrated circuits, silicon carbide (SiC) and its power transistors, gallium nitride (GaN), diamond, etc.